Babeș-Bolyai University Cluj-Napoca

Faculty of Environmental Science and Engineering

Application of gamma and alpha spectrometry for a quantitative assessment of environmental radionuclides in various sedimentary records such as lakes, peat bogs and loess

Kelemen Szabolcs

-Ph.D Thesis summary-

Scientific coordinator: Prof. Dr. Alida Gabor (Timar)

Cluj-Napoca 2023

Keywords

Alpha spectrometry, gamma spectrometry, ^{210}Pb dating method, sediment, peat, loess, mobility, ^{210}Pb/^{226}Ra disequilibrium

Table of contents

1.Introduction

The aim of this doctoral thesis is to investigate the natural occurrences of radionuclides and their determination in various environmental samples, such as sediments, peat bogs, and loess, while examining the temporal changes and applications of radionuclides in the study of human activity's impact on the environment using diverse methodologies and sample types. Furthermore, this thesis explores the mobility of radionuclides, the implications of radioactive disequilibrium, and the optimization of chemical digestion techniques for improved sample analysis, with particular emphasis on the ^{210}Pb method.

The thesis is organized into several sections, beginning with an introduction chapter, which is then followed by **Chapter II (Gamma and alpha spectrometry)** that provides the description of the Gamma and Alpha spectrometry equipment, and their utilization in the determination of activity concentration of radionuclides in environmental samples. In addition, this chapter includes the techniques involved in the preparation of environmental samples, as well as the description of the principles of the ^{210}Pb dating method.

The aim of the studies presented in **chapter III (Examination of the ^{210}Po, ^{210}Pb and ^{137}Cs isotopes mobility in the sediments column under different chemical condition)** was to provide new insights into the mobility of ^{210}Po, ^{210}Pb, and ^{137}Cs isotopes in sediments under different chemical conditions and their impact on the accuracy of the ^{210}Pb dating method. Specifically, the changes in ^{210}Po mobility in sedimentary environments in relation to changes in pH, Cl^-, and $NO3^-$ concentrations were examined, to identify factors that influence the accuracy of the ^{210}Pb dating method. This work is noteworthy for its comprehensive examination of ^{210}Po behavior in artificial sediment columns and under various chemical conditions. The findings have contributed to improving the accuracy of the ^{210}Pb dating method, enabling more reliable estimates of sedimentation rates. Furthermore, the research has contributed to a better understanding of the scientific community on radionuclide mobility.

The aim of the **chapter IV (Application of the ^{210}Pb chronology method on the central Danube Delta lake system)** is to showcase the changes in sediment dynamics in the central region of the Danube Delta, a UNESCO World Heritage site, by analyzing four lakes and twelve sediment cores using the ^{210}Pb chronology method. Sediment dynamics of the central part of the Danube

Delta before and after the construction of the Iron Gates is examined. The study sheds light on the impact of human interventions, particularly the Iron Gate Hydro-Energetic Power Plants, on the Delta's environment. The hypothesis of this study is that the construction of the Iron Gates has had a significant impact on sediment dynamics in the Delta, leading to decreased sediment delivery and severe coastal erosion. The research provides new insights into sediment dynamics that can be widely utilized in future studies. The results of this chapter can help in achieving a better understanding of the impacts of human interventions on sediment dynamics in the Danube Delta and contribute to the development of more effective management strategies for the conservation of this unique ecosystem. The present chapter draws upon two published scientific articles (Begy et al, 2018, a, b).

In **Chapter V (Improving digestion methods for the determination of ^{210}Po by alpha spectrometry from peat bog samples)** we investigate and establish an optimal approach for the digestion of peat bog samples, with the aim of producing alpha sources of polonium that exhibit favorable spectral characteristics and yield maximum deposition efficiency within a minimal timeframe. Four different digestion procedures that employed various combinations of nitric acid, hydrochloric acid, hydrofluoric acid, hydrogen peroxide, and thermal digestion, with a traditional method commonly used in the scientific literature are compared. Based on these results, it is possible to significantly reduce digestion time with one of the methods by up to a few hours. This research contributes to improving the efficiency of analyzing peat bog samples. The results are currently submitted for publication (Kelemen et al., submitted).

The aim of the **Chapter VI (Application of the gamma and alpha spectrometry methods for the determination of a natural radionuclides in loess samples)** was to examine the relationship among various natural radionuclides in loess sediments by using gamma spectrometry. The study employed gamma spectrometry to determine the activity concentrations of radionuclides (^{210}Pb, ^{238}U, ^{232}Th, ^{226}Ra and ^{40}K) in eight loess deposits situated in the regions of the United States, Europe and China. The study also addresses radioactive equilibrium between ^{222}Rn and ^{226}Ra, which is observable in all loess samples. In cases where equilibrium is not observed we show that the difference in the specific activities measured for ^{210}Pb and ^{226}Ra in loess samples is not due to measurement errors but rather the result of ^{222}Rn diffusion. This can have an impact on the accuracy of the Optically Stimulated Luminescence (OSL) method for determining

the age of loess layers. Therefore, these results may have great significance for the more accurate determination of the age of loess layers. These gamma and alpha spectrometry results presented here served for the calculation of the ages of the loess layers presented in two peer reviewed publications (Constantin et al., 2019, Avram et al., 2020).

At the end of the dissertation **Conclusions** are presented.

2. Gamma and alpha spectrometry

2.1 Gamma spectrometry

Radionuclide content measurements were carried out using an ORTEC Digidart gamma spectrometer with an ORTEC GML HPGe Coaxial Well semiconductor detector (FWHM at 1.33MeV of 1.92KeV with 0.1 mm Al window for low energies, with 4 π geometry high absolute counting efficiency for small samples) having a passive shielding of 10 cm thick lead and 3 cm copper "Sarpagan" type geometry was used with a cylindrical tube with adequate dimensions. Samples were put into plastic tube and stored for at least 21 days to ensure the equilibrium between ^{222}Rn and ^{226}Ra. The Maestro-32 gamma software was used to analyze the peaks of interest: ^{210}Pb at 46.5 keV, ^{238}U at 63 keV, 92 keV, ^{232}Th 238 keV, 338 keV, 583 keV, ^{137}Cs at 661 keV, ^{226}Ra (for $^{210}Pb_{sup}$) through ^{214}Pb at 295 keV and 351 keV, and through ^{214}Bi at 609 keV.

2.2 Alpha spectrometry

Chemical separation was employed as described in the following sections to isolate the radionuclides of interest prior to measurement of samples. Alpha spectrometric measurements were conducted utilizing an Ortec Soloist PIPS detector with a resolution of 19 keV. The ASPEC-927 Dual Multichannel was utilized for data acquisition. The detection limits for ^{209}Po and ^{210}Po are expressed in units of Bq kg^{-1}. The Maestro32 software was utilized to acquire spectra, and activity concentrations were determined by subtracting the background from the previous measurements.

2.3 ^{210}Pb chronology

The ^{210}Pb radioactive-dating technique, based on the radionuclide`s half-life of 22.3 years, is commonly employed to determine short-term peat bog growth rates, sediment deposition, and

sedimentation rates (0-200 years) in various aquatic environments such as oceans, estuaries, rivers, and lakes. This method is considered highly reliable and frequently used due to the extended half-life and relative insolubility of ^{210}Pb. The accumulation rate or flux of ^{210}Pb, as established by Appleby and Oldfield in (1978), enables the reconstruction of sedimentation rate variations over time. Being a constituent of the ^{238}U decay series, this naturally occurring radioactive element can be found in both terrestrial sediments and the aerial environment. The sedimentary ^{210}Pb can be attributed to two distinct sources. Firstly, the supported ^{210}Pb, which undergoes continuous decay in the sedimentary environment, originates from its parent radionuclide, ^{226}Ra, and these are assumed to be in a state of secular equilibrium. Secondly, the unsupported ^{210}Pb is produced by the emanation of ^{222}Rn from soils, which subsequently undergoes decay into a series of short-lived radionuclides. These radionuclides are ultimately deposited in the catchment area and directly in the lake.

Various ^{210}Pb dating models based on several assumptions related to the initial activities of ^{210}Pb, ^{210}Pb flux or accumulation rate (Appleby and Oldfield, 1978) exist, which make it possible to reconstruct variations in the sedimentation rate throughout time. The model used in this study is the Constant Rate of Supply model (CRS) (also known as Constant Flux model – CF). It has as fundamental hypotheses an efficient transfer from the water column to the sediments and a constant $^{210}Pb_{ex}$ flux of the sediment surface and no diffusion throughout time. The chronologies are generated by comparing the overall core ^{210}Pb inventory to partial inventories below depth i, by integrating the supported ^{210}Pb concentration, the bulk density and the thickness of each sediment layer, obtaining the mass sedimentation of each layer and the ages at the limit of the sediment layers (Mabit et al., 2014). The mass accumulation rates and the initial $^{210}Pb_{ex}$ concentrations may change over time in the layers, but must be inversely proportional (Appleby, 2001). The increase of sediment supply does not always imply the higher $^{210}Pb_{ex}$ fluxes in the upper sediment layer. In other words, the sedimentation rate and the initial $^{210}Pb_{ex}$ concentration can be variable or irregular throughout time.

The accumulated deposit below the layer i can be written as:

$$A_i = A_0 e^{-\lambda t} \qquad (2.1)$$

The age of the layer i can be calculated as follows:

$$t_i = \frac{1}{\lambda} \ln \frac{A_0}{A_i} \qquad (2.2)$$

The mass accumulation rate for layer i can be calculated using:

$$r_i = \frac{\lambda A_0 e^{-\lambda t}}{C_i} = \frac{\lambda A_i}{C_i} \qquad (2.3)$$

The CRS model can be and has been validated by several independent methods and is therefore the most applied dating method. It can be used if sedimentation rates vary significantly and if the sediment was prone to mixing (Szarlowicz et al., 2013).

3. Examination of the ^{210}Po, ^{210}Pb and ^{137}Cs isotopes mobility in the sediments column under different chemical condition

The ^{210}Pb dating method is commonly employed to establish chronologies and sedimentation rates in aquatic environments. The ^{210}Pb dating method assumes that the ^{210}Pb flux to the sediment is constant and that the ^{210}Pb activity in the sediment decreases exponentially with depth due to radioactive decay. This method may be affected by several factors that can alter the ^{210}Pb distribution in the sediment, such as bioturbation, erosion, deposition, and chemical processes. One of the potential sources of error in the ^{210}Pb dating method is the mobility of ^{210}Po, the alpha-emitting daughter of ^{210}Pb. ^{210}Po is produced through the decay of ^{210}Pb in sediment, but it can migrate between layers in a soluble form. This migration can lead to errors in estimating the ^{210}Pb age. Understanding ^{210}Po's behavior in different sedimentary environments is crucial for accurately applying the ^{210}Pb dating method. (Sanchez-Cabeza et al. 2012, Barsanti et al. 2020)

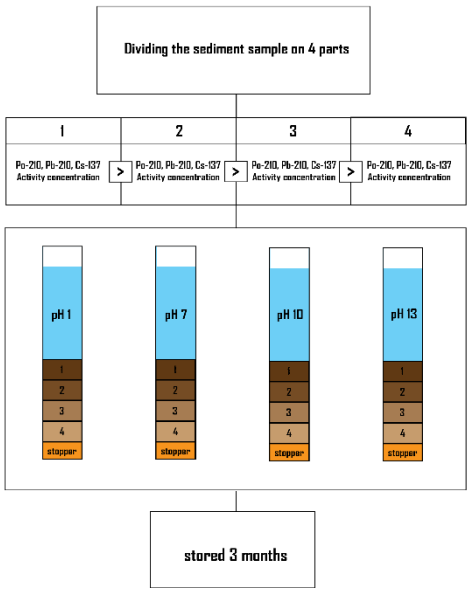

Figure 3.1. Sediments column preparation

The study examined the mobility of ^{210}Po, ^{210}Pb, and ^{137}Cs isotopes in sediment columns under different chemical conditions. The ^{210}Pb dating method, commonly used for establishing sediment chronologies, assumes a constant ^{210}Pb flux and exponential decrease with depth. However, the mobility of ^{210}Po, the daughter of ^{210}Pb, can introduce errors in the dating method. The study aimed to understand the behavior of ^{210}Po and its impact on the ^{210}Pb dating method. Four sediment columns with known concentrations of ^{210}Pb, ^{210}Po, and ^{137}Cs were exposed to different chemical conditions (**Figure 3.1).**

After three months, the columns were sliced, and radionuclide concentrations were measured. The results showed that ^{210}Po exhibited significant variations in concentration depending on the pH of sediment layers. It was more soluble and mobile in acidic conditions, while being adsorbed and immobilized in neutral and alkaline conditions. ^{210}Po shows significant variations in concentration depending on the pH and the layer. In particular, the 3->4 layer of the sample with pH 1 shows a high migration of ^{210}Po, with about 35 Bq/kg (40% of the initial activity) moving to the lower layers (**Figure 3.2).** The study concluded that ^{210}Pb is relatively stable and can be used for dating sediment accumulation rates, but ^{210}Po mobility should be considered, especially in low pH conditions, to avoid underestimation of ^{210}Pb activity and sedimentation rates. Environmental factors influencing ^{210}Po distribution should be taken into account when using the ^{210}Pb dating method.

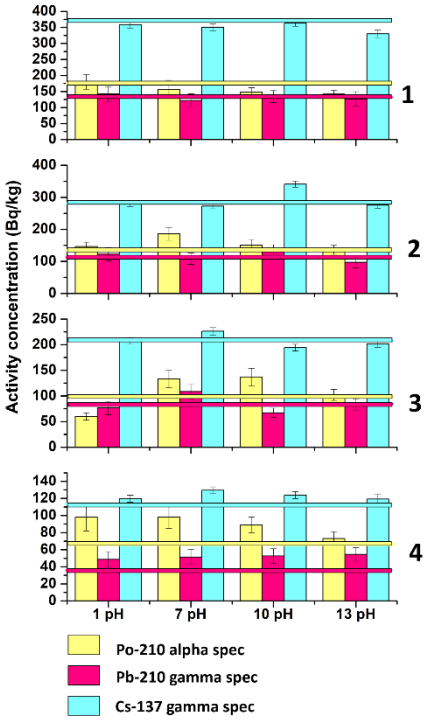

Figure 3.2. ^{210}Pb, ^{210}Po and ^{137}Cs activity concentration in different layers with different pH environment

4. Application of the ^{210}Pb chronology method on the central Danube Delta lake system

This study examines sediment dynamics in the central part of the Danube Delta, focusing on the period before and after the Iron Gates' construction to understand its effects, by analyzing 4 lakes and 12 sediment cores and pointing out the period before and after the construction of the

Iron Gates. The Iron Gate Hydro-Energetic Power Plants, built in 1972 and 1986, greatly influence the delta's sediment content by trapping large amounts of sediment, disrupting natural sediment flow, and causing coastal erosion. (ICPDR, 2015, Laszlo, 2007). This impact is evident in the decreasing solid discharge of the Danube River from 1971 to 1990 (Coman, 2002).

4.1 Study site

From the central part of the Danube Delta (**Figure 4.1.**) between the Saint Gheorghe and Sulina branches four lakes were sampled, namely: Iacob, Cuibida, Isac and Uzlina. Iacob Lake is part of the Rosu-Puiu lake complex and has a total surface area of 2208 ha.

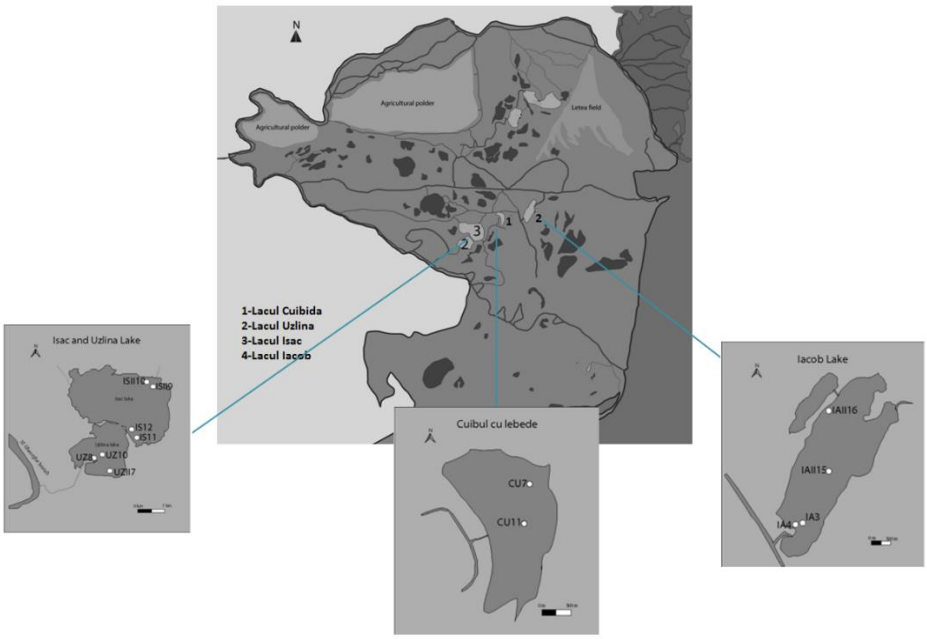

Figure. 4.1. Iacob, Cuibida, Isac and Uzlina lake and the location of the sampled sediment cores

4.2 Materials and methods

The sediment cores were sliced into 1-3 cm sections for sub-sampling and dried in an oven at 75°C. The sub-samples, weighing 2-5 g, were used to measure physical properties like bulk density, water content, and porosity (Saravana Kumar et al., 1999). The remaining sub-samples were dried, ground, sieved, and stored for spectrometric measurements. LOI measurements at different temperatures determined organic mass (OM) and carbonate content (IOC), which together gave the total carbon content (TOC).

Heavy metal concentrations were measured using an Inductively Coupled Plasma Mass Spectrometer of the SCIEX Perkin-Elmer Elan DRC II type. The exact measurement method described in Baceva et al. (2011) was used for heavy metal determination.

4.3 Results and discussion

Iacob lake

Hakanson (1977) observed a correlation between the OM and Water content of the sediments when analyzing the Swedish Lake Akoln. This connection is evident in the sediments of Lake Iacob, with the exception of the IA3 core, where the water content does not increase in the same manner as the OM. The deposition of inorganic matter was higher than that of the OM, and the pressure in the upper layers was lower than that of the lower ones. The mean ^{226}Ra concentration had an average of 20±2 Bq/kg in the cases of IA3, IA4, and IAII15, while in the case of IAII15 it was only 15±2 Bq/kg. The ^{210}Pb concentration decreased according to the law of disintegration, some perturbation being visible throughout the sediment cores. The dating horizons were taken at 49 cm for IA3, 55 cm for IA4, at 69 cm for IAII15 and at 37 cm for IAII16. **(Figure 4.2)**

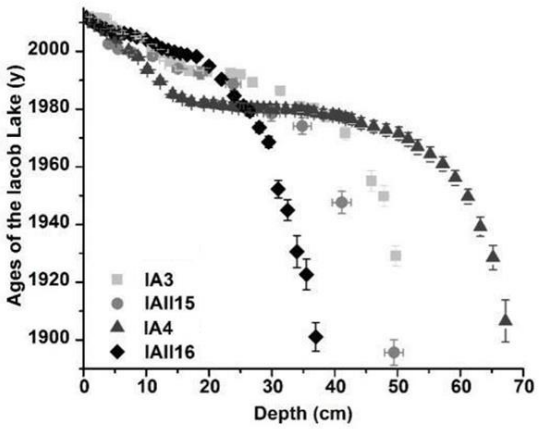

Figure. 4.2 The ages of the Iacob Lake core

Figure 4.3 shows a correlation between the depth of sediment cores and age distributions. The data reveals two discernible ^{137}Cs peaks, one in 1986 (attributed to the Chernobyl nuclear accident) and the other in 1963 (associated with nuclear weapon tests). The ^{137}Cs contamination originating from the Chernobyl nuclear accident is relatively low, but the thermonuclear weapon test with maximum ^{137}Cs contamination in 1963 caused general, evenly spread contamination throughout the entire catchment area. The sampling points situated in the vicinity of the main inflow channel and the one situated at the secluded shore show similar increases in cumulative mass, reaching values in the 27-32 g cm^{-2} yr^{-1} range, while the one situated in the middle of the lake (IAII15) receives the least quantity of sediment (17 g cm^{-2} yr^{-1}).

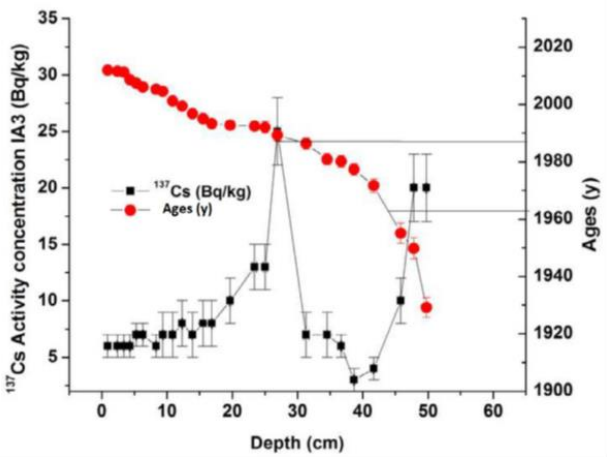

Figure. 4.3 The ^{137}Cs activity concentrations in the IA3 core

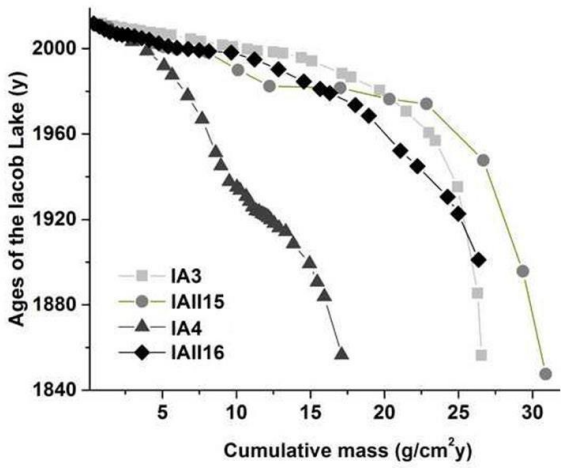

Figure. 4.4 The cumulative masses of the Lake Iacob cores

Iacob lake heavy metal concentration

Heavy metal concentration measurements were conducted on the IA3 sediment core in the south, at the main inflow of the lake. The average concentrations were 16.933 ppm Li, 3.955% Mg, 10.726% Al, 2.275% K, 28.554 ppm Cr, 291.408 ppm Mn, 14.09% Fe, 6.006 ppm Co, 14.924 ppm Ni, 22.883 ppm Cu, 8.289 ppm As, 401.883 ppb Cd, and 245.45 ppb Hg. In the case of Zn and Pb, half the measured samples were below the limit of detection, their highest values being 78.469 ppm and 11.575 ppm respectively.

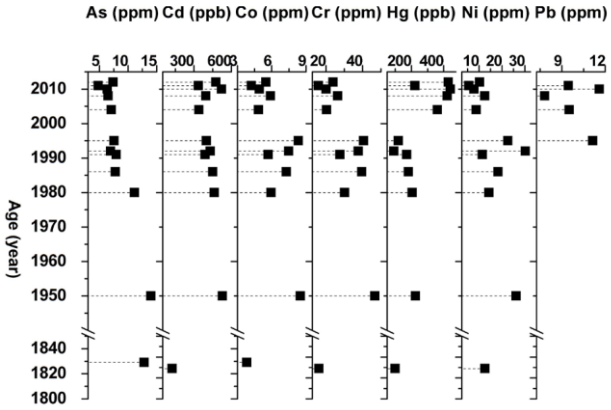

Figure 4.5 Heavy metal concentration in the IA3 core

As, Cd, Co, Cr, Hg and Ni started to appear in 1980, when the Danube Delta received a great amount of sediment (confirmed by the high sedimentation rates in the 1974–1982 period) (**fig.4.5**). The metallurgical industry in Romania was the most flourishing in the 1950–1982 period, when 6 metallurgical factories were constructed, one of them being at the edge of the Danube Delta, in Tulcea Slatina. The decreasing heavy metal content in the 1990s can be an indicator of the failure of industrial production due to political changes in eastern Europe and Romania. Hg and Pb concentrations were increasing in the upper layers of the sediment core, while Cr, Co and Ni showed lower values compared to the 1.45

times higher values registered in the 1980–1995 period. As concentrations showed a decreasing trend compared to the 14 ppb measured in the marine substrate, reaching 4 ppm by 2013. The average content of As in soil on the Earth was 6.8 ppm.

Cuibida Lake

Two sediment cores were taken from the Cuibida Lake, and an 28% organic matter (OM) peak is visible (**figure 4.6**). The exponential profile of ^{210}Pb according to depth is visible in both cores, with some minimums (**figure 4.7**). The distribution of ages according to depth shows that the CU7 sampling point is subjected to a more serious sedimentation than CUII11. A total of 27 cm sediment was deposited in the past 100 years in the CUII11 point, while the same amount was deposited at the entrance of the north-eastern channel (CUII11) over a period of 10 years. A plateau was formed in case of CU7 in the age-depth distribution after 2000 and, until 2013, 40 cm sediment was deposited, meaning a 3 cm y^{-1} linear sedimentation (**figure 4.8**).

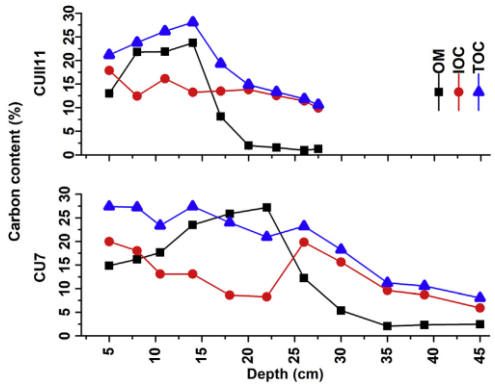

Figure 4.6 The carbon content of the Cuibida Lake cores

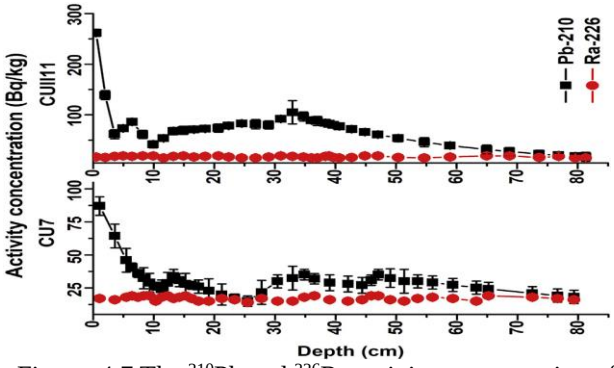

Figure. 4.7 The ^{210}Pb and ^{226}Ra activity concentration of the Cuibida Lake cores

The high sedimentation of this sampling point can be explained with its localization and frequency of floods on the Sulina Branch. The ^{137}Cs activity concentration of the CU7 core can be seen in **figure 4.8**. Cesium measurements were carried out for all sediment cores and the values for the ^{210}Pb and ^{137}Cs were in good agreement. Average mass sedimentation rates are 0.51 g cm^{-2} y^{-1} for CU7 and 0.43 g cm^{-2} y^{-1} for CUII11. Drastic increasing can be observed after 1989, where the 14-year average increased on average from 0.38 ±0.06 g cm^{-2} y^{-1} to 0.68 ±0.10 g cm^{-2} y^{-1} (**figure 4.9**)

The peaks of 2006 and 2011 are visible in both organic and inorganic sedimentation and show similar tendencies, proving that the carbon content of the sediment arrives simultaneously with the sediment and is not present due to the decay of the vegetation. In the 1988–2004 period, the sediment containing carbon is second to the non-carbon one, the first having a sedimentation of 0.05 g cm^{-2}, while the second is in the 0.4–0.8 g cm^{-2} range.

Isac Lake

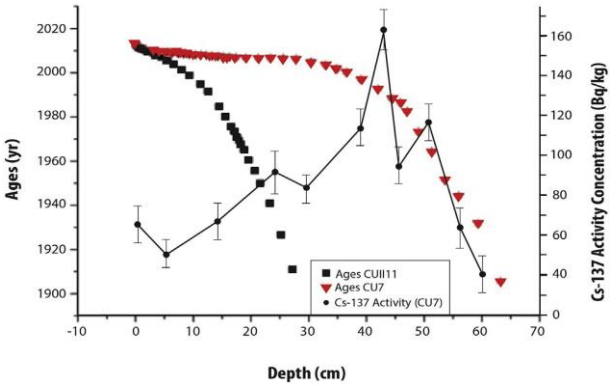

Figure. 4.8 The age depth model and ^{137}Cs activity concentration for Cuibida Lake cores

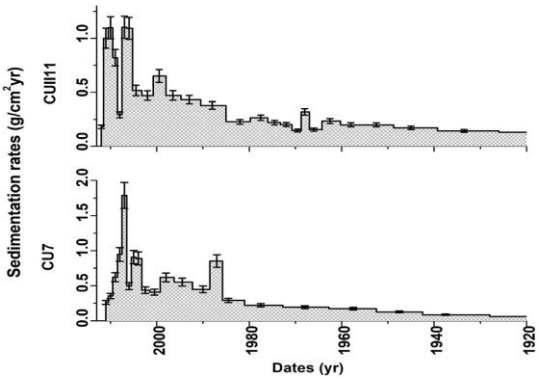

Figure. 4.9 sedimentation rates of the Cuibida Lake cores

According to the sampling areas, the four sampled cores can be grouped into two groups: samples ISII9 and ISII10 from the northeastern part of the lake, close to the entry channel, and IS11 and IS12 from the south-eastern part, close to the inflow channel.

In the case of IS12 and ISII9, the ^{226}Ra concentration had an average of 30 ± 4 Bq/kg, while in the case of IS11 and ISII10 this value was lower: 13±2 Bq/kg. The latter two sampling points were in the proximity of the inflow channels and a greater ^{226}Ra quantity could be dissolved. The dating horizons were taken at 34 cm for IS11, at 75 cm for IS12, at 65 cm for ISII9 and at 51cm for ISII10 **(figure 4.10).**

In the case of IS11, the mean sedimentation is 0.45 g cm^{-2} yr^{-1}, while in the case of IS12, the mean sedimentation is 0.82 ±0.07 g cm^{-2} yr^{-1}. The IS12 sediment core is prone to an increasing sediment deposition tendency starting from the 1980's, having a series of local maximums. The Mahmudia Meander straightening (1984–1988) increased the sediment intake to almost double in

1986. The first ten years for the ISII10 core show a decreasing from 0.86 ±0.12 g cm^{-2} yr^{-1} to 0.13± 0.01 g cm^{-2} yr^{-1} by the 1950's **(figure 4.11)**

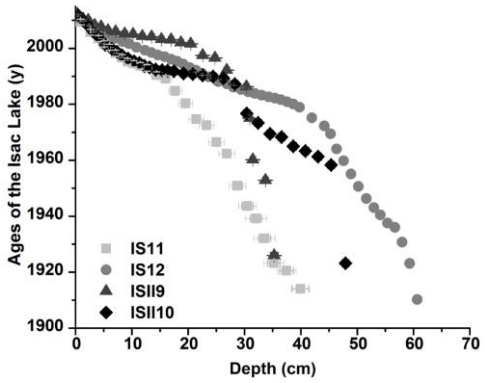

Figure 4.10 The ages of the lake Isac cores.

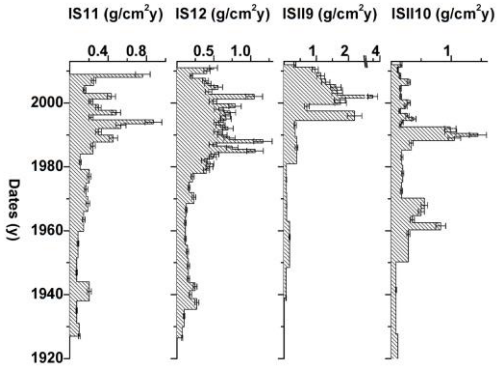

Figure 4.11 The mass-sedimentation rates of the lake Isac cores

In 1991, the sedimentation decreases to a minimum of 0.14 g cm^{-2} yr^{-1}. The sedimentation rate of Lake Isac has increased significantly since 1989, with a maximum of 3.95 ±0.06 g cm^{-2} yr^{-1} being found in 2002. The lake has a high biomass content and intense vegetation in the areas of the sampled cores, with the OM content being commensurately high. After the first 15 cm of the ISII10 core, a plateau is visible, which points to a great influx of sediment over a 2 year time span. In the ISII9 core, the extent of compaction decreases with the OM content. In the IS12 core, a compaction, together with the increase of OM, is also evident.

The most sediment was deposited in the area of the IS12 core, which points to greater exposure. Five peaks are visible: in 2014, 2001, 1998, 1991–1994 and 1988. The deposited mass sedimentation quantity in the IS12 core shows that the 1991–1993 flooding period was the most significant (0.82 ±0.07 g cm^{-2} yr^{-1}). In the ISII9 core, the mass sedimentation rate increased sharply to 0.51±0.06 g cm^{-2} yr^{-1} from 0.06±0.01 g cm^{-2} yr^{-1}. In the ISII10 core, the sedimentation rate decreased drastically to 0.13 ±0.01 g cm^{-2} yr^{-1} from 0.86+0.12 g cm^{-2} yr^{-1} recorded ten years before.

After the 1970s, the sedimentation rate decreased from 0.61±0.14 g/ $cm^{-2}y^{-1}$ to 0.22±0.03 g cm^{-2} yr^{-1}. The increases in the ISII9 sedimentation rates happened simultaneously with the decreases of the sedimentation rates in the ISII10 sampling point. This could have been due to the

fact that until the 1990s the western part of the entrance to the north-eastern channel was more exposed to sediment deposition.

Uzlina lake

The three sediment cores analyzed from the Uzlina Lake have the highest organic material content (between 19% and 38%) (**figure 4.12**), being situated in an area near the inflow-channels. The most affected areas are those near the inflow-channels, with most flooding events recorded by UZ8 and UZ10 in the periods of 1995–1996, 1999–2000, 2005–2006, and 2008–2010. The decreasing effect on sedimentation of the Iron Gate's construction can be observed in the UZ8 and UZII7 cores situated near the inflow channel, while its effect is not visible on the UZ10. This can be caused by a series of factors such as the location of the sampling point and the local natural and anthropogenic influences.

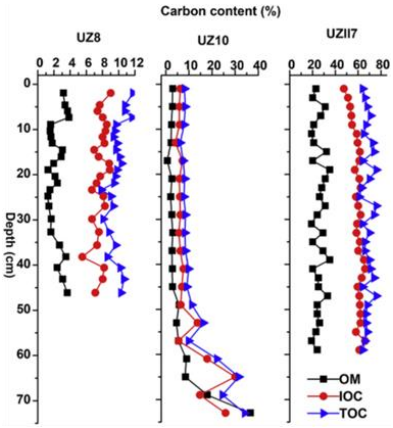

Figure 4.12 The carbon content of the Uzlina Lake cores

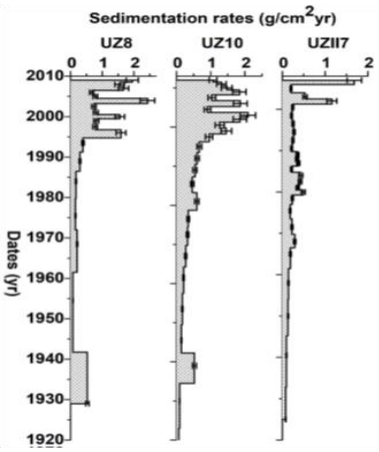

Figure 4.13 sedimentation rate of Uzlina lake cores

The mean sedimentation of the lake (0.26 ±0.02 g cm^{-2} yr^{-1}) in the period of 1940–1972 decreases 16% in the period of 1972–1980. The sedimentation rate increases drastically after the 1980's, which could have been majorly influenced by the straightening of the Mahmudia Meander (1984–1988) and the increased lumbering. The mean sedimentation rate (0.27 ± 0.02 g cm^{-2} yr^{-1}) calculated for the 1972–1989 period increases 4 times in the 1989–2013 period (1.00 ± 0.10 g cm^{-2} yr^{-1}) (**figure 4.13**).

5. Improving digestion methods for the determination of ^{210}Po by alpha spectrometry from peat bog samples

This research aims to determine the ideal strategy for peat bog digestion in order to obtain polonium alpha sources with good spectral features and the optimum yield from the deposition process in the shortest amount of time. To achieve this, four different digestion processes were compared to a common digestion method, which was frequently utilized in the scientific literature (Figgins 1961, Miley 2009, Seiner 2014, Flynn 1968). A stainless steel disc was employed for the spontaneous deposition.

5.1 Materials and methods

A peat core was collected in 2018 from Violeta peatland (Vio) in the Latoritei Mountains. Four subsequent peat bog layers were used for the investigation of chemical digestion methods, namely Vio 1.1, Vio 1.3, Vio 1.5, Vio 1.8, and Vio 1.11.

The traditional method for extracting polonium from samples involves using two types of acids: concentrated nitric acid (NHO_3) and hydrochloric acid (HCl). The sample is dissolved in concentrated nitric acid, then further dissolved in hydrochloric acid. The process also includes the use of peroxide (H_2O_2) to destroy organic matter. Beside this method four other methods were tested.

Method I dissolves the peat bog sample in nitric acid (HNO_3) and hydrochloric acid (HCl) at 80°C, excluding hydrogen peroxide (H_2O_2).

Method II introduces hydrogen peroxide (H_2O_2) and hydrochloric acid (HCl) to the peat bog sample at room temperature, reducing the final solution volume to 5 ml.

Method III incorporates nitric acid (HNO_3), hydrofluoric acid (HF), and boric acid (H_3BO_3) in a Teflon beaker at 80°C, concluding with the addition of hydrogen peroxide (H_2O_2).

Method IV digests the organic portion of the peat bog sample at 300°C for three hours, then applies hydrochloric acid (HCl) and hydrogen peroxide (H_2O_2) to the residual ash.

Polonium alpha sources were prepared using the method published by Begy (2014). Measurements were taken with an Ortec Soloist alpha spectrometer with a PIPS detector 900 mm^2 and data collected using an ASPEC-927 Dual Multichannel.

Preparation for alpha spectrometry is time and effort intensive, and the accuracy of the approach can be significantly impacted by the quality of the experimental procedure. Five samples of peat bog (Vio 1.1, Vio 1.3, Vio 1.5, Vio 1.8, Vio 1.11) were tested using the aforementioned chemical digestion techniques. The duration time of each technique was recorded. To ensure comparability, the control method was validated using IAEA 447 reference sample. The polonium recovery was found to be approximately 84.1% for ^{209}Po and 81.8% for ^{210}Po (**table 5.1**). The control digestion method was used to digest the Vio peat bog samples and obtained ^{210}Po activity concentrations. These values were then compared to ^{210}Po activity concentrations obtained by various digesting methods. According to the activity concentration presented in **figure 5.1**, the levels of uncertainty that are greatest for procedures III and IV of chemical digestion, however the values are consistent.

Sample		^{210}Po Masured Value		^{210}Po Refrence Value		Diff %
ID		(Bq/kg)		(Bq/kg)		(%)
	1	288.6	±17.0	311	±16.0	-7.2
IAEA	2	296.7	±17.2	311	±16.0	-4.6
447	3	286.1	±16.8	311	±16.0	-8.0
	Avg	298.9				93.2
	SD	6.3				2
	SEM	±3.6				±1.2

Table 5.1. Validation of the control digestion method with IAEA-447 reference

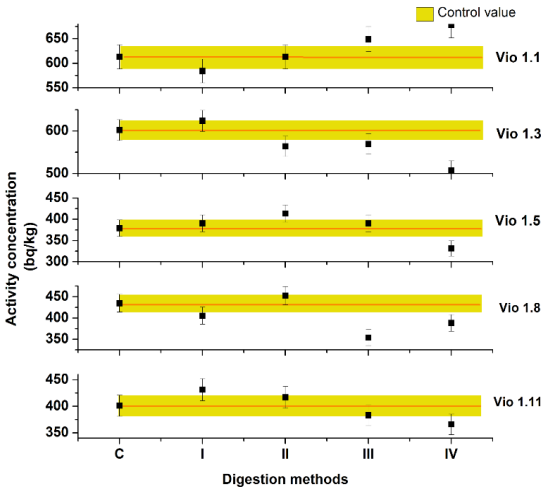

Figure 5.1. Comparison of the ^{210}Po activity concentration

It is possible that ^{209}Po and ^{210}Po will not be released from the matrix in the same proportion. As a consequence of this possibility, there may be some degree of uncertainty associated with the III and IV procedures.

The average of their results obtained by different digestion methods were compared with the average of the reference value by dividing them by reference value and looking at how much they deviate from one (**figure 5.2, fable 5.2**).

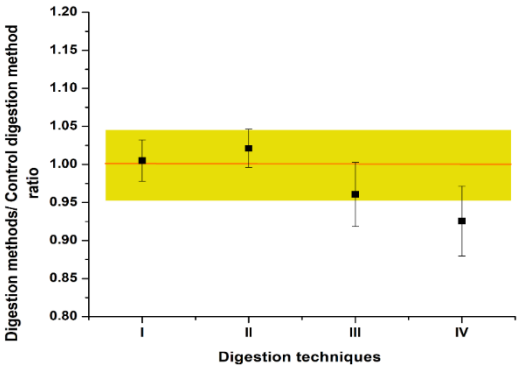

Figure 5.2. Digestion method ratio compared to the control method

Sample	Control method		Method I		Method II		Method III		Method IV	
ID	^{210}Po (Bq/kg)		^{210}Po (Bq/kg)		^{210}Po (Bq/kg)		^{210}Po (Bq/kg)		^{210}Po (Bq/kg)	
Vio 1.1	613	±25	584	±24	613	±25	649	±25	678	±26
Vio 1.3	602	±25	624	±25	564	±24	569	±24	508	±23
Vio 1.5	379	±19	390	±20	413	±20	390	±20	331	±18
Vio 1.8	435	±21	405	±20	453	±21	354	±19	388	±20
Vio 1.11	401	±20	431	±21	417	±20	383	±20	366	±19
	Control/Control ratio		I/Control ratio		II/Control ratio		III/Control ratio		IV/Control ratio	
Vio 1.1	1	±0.04	0.95	±0.04	1	±0.04	1.06	±0.04	1.11	±0.04
Vio 1.3	1	±0.04	1.04	±0.04	0.94	±0.04	0.95	±0.04	0.84	±0.04
Vio 1.5	1	±0.05	1.03	±0.05	1.09	±0.05	1.03	±0.05	0.87	±0.05
Vio 1.8	1	±0.05	0.93	±0.05	1.04	±0.05	0.81	±0.05	0.89	±0.05
Vio 1.11	1	±0.05	1.08	±0.05	1.04	±0.05	0.96	±0.05	0.91	±0.05
Avg	1	±0.05	1.01	±0.03	1.02	±0.03	0.96	±0.04	0.93	±0.05
SD			0.06		0.06		0.1		0.1	
SEM			±0.03		±0.03		±0.04		±0.05	

Table 5.2. Comparison of the chemical digestion method results

Method I: The result was extremely near to the value that was used as a reference, with the maximum amount of positive variance being 0.5%. The duration of the chemical digestion process was 24 hours.

The result from Method II exceeded the reference value and had a positive deviation that was marginally significant (2.1%). Digestion by chemical processes takes 4 hours.

Method III produced a result that was below the reference value and had a moderately negative deviation of -3.9%. The duration of the chemical digestion process equals 28 hours.

Method IV: The result was a significant amount below the reference value, with a considerable percentage of departure in the negative direction (-7.4%). The duration of the chemical digestion process equals 24 hours.

The ^{209}Po recovery of the different chemical exploration methods was determined by comparing the ^{209}Po (30 mBq=100%) tracer activity with the measured ^{209}Po activity. In this the efficiency (28-34%) of the PIPS detectors was taken into account.

Sample	Control method		Method I		Method II		Method III		Method IV	
ID	^{209}Po yield (%)		^{209}Po yield (%)		^{209}Po yield (%)		^{209}Po yield (%)		^{209}Po yield (%)	
Vio 1.1	86.8	±4.6	71.4	±4.2	73.4	±4.1	72.7	±4.1	59.1	±3.8
Vio 1.3	75.5	±4.3	78.5	±4.1	63.0	±3.8	63.6	±3.8	59.5	±3.9
Vio 1.5	84.1	±4.6	69.9	±4.0	62.7	±3.8	69.7	±4.0	52.6	±3.6
Vio 1.8	83.2	±4.6	67.7	±4.1	64.5	±3.8	69.1	±4.0	65.8	±4.1
Vio 1.11	79.3	±4.2	75.3	±4.3	73.9	±4.1	70.8	±4.1	61.9	±3.9
Avg	81.8		72.6		67.5		69.2		59.8	
SD	4.4		4.3		5.7		3.4		4.8	
SEM	2.0		1.9		2.5		1.5		2.2	
Digestion time (h)	**72**		**24**		**4**		**28**		**12**	
Deposition time (h)	3		3		3		3		3	

Table 5.3. ^{209}Po chemical recovery used different digestion methods

The most acceptable activity concentrations were obtained from samples subjected to chemical digestion methods I and II. The results did not exhibit significant deviation from those obtained using control digestion methods. The ^{209}Po tracer was used as an indicator of the chemical recovery of each method. The results showed that Control Method and Method I had the highest ^{209}Po recovery rates (81,8% and 72.6%, respectively), while Method IV had the lowest (60%). Methods I and III had significantly higher ^{209}Po recovery rates than Methods II and IV. None of the methods reached or surpassed the ^{209}Po recovery rate of the Control method. The duration of each method varied from 4 hours (Method II) to 28 hours (Method III). Based on these findings, the conclusion is that Methods I and II were the most accurate and reliable chemical digestion methods for peat bog samples, while Method IV was the least accurate and reliable. Method II had the additional advantage of being faster than Methods I. Therefore, we recommend Method II as the optimal chemical digestion procedure for peat bog samples for ^{210}Po alpha spectrometry measurements.

6. Application of the gamma and alpha spectrometry methods for the determination of a natural radionuclides in loess samples

Loess, prevalent Quaternary sediment, is a crucial resource for understanding past climatic and environmental shifts (Raymond 2015). This study uses gamma spectrometry to examine the activity concentrations of certain radionuclides in loess samples from the USA, Europe, and China. These radionuclides help determine annual doses received by the samples, essential in luminescence dating. The analysis also observes imbalances in the decay series, particularly between the parent element ^{226}Ra and its daughter ^{210}Pb, caused by the system's exhalation of ^{222}Rn.

6.1 Results

The **table 6.1.** and **figure 6.1a** show the descriptive statistics of the activity concentration of ^{210}Pb, ^{238}U, ^{232}Th, ^{226}Ra and ^{40}K in eight loess depositions from different regions of the world. The activity concentration is expressed in Bq/kg and the error is given as the standard deviation. The loess cores are identified by their abbreviations: MV (Romania), RS (Romania), ROX (Ukraine), STY (Ukraine), BAT (Serbia), KUM (USA), END (USA) and BCY (China).

The table reveals some interesting patterns and variations in the radionuclide activity concentration among the loess cores. For example, ^{210}Pb has the highest activity concentration in STY (25.1 Bq/kg) and the lowest in RS (15.5 Bq/kg). ^{238}U has the highest activity concentration in BAT (40.5 Bq/kg) and the lowest in KUM (26.2 Bq/kg). ^{232}Th has the highest activity concentration in KUM (43.5 Bq/kg) and END (42.8 Bq/kg) and the lowest in STY (31.9 Bq/kg). ^{226}Ra has the highest activity concentration in KUM (44 Bq/kg) and END (43.4 Bq/kg) and the lowest in BCY (34.8 Bq/kg). ^{40}K has the highest activity concentration in KUM (629.2 Bq/kg) and END (623.5 Bq/kg) and the lowest in ROX (391.3 Bq/kg).

Loess deposits		^{210}Pb Bq/kg		^{238}U Bq/kg		^{232}Th Bq/kg		^{226}Ra Bq/kg		^{40}K Bq/kg	
		Act	Err ±	Act	Err ±	Act	Err ±	Act	Err ±	Act	Err ±
Mircea Vodă (RO)	max	35.3	5.3	46	3	46.6	0.6	43.3	1.6	455.7	15.3
	min	12.6	2.3	28.5	5.3	34.3	1.3	33.7	1.7	368.6	16.1
	Avg	22.5	1.5	36.7	1	38.2	0.8	39.1	1.5	404.7	5.7
	SD	6.6		4.4		3.7		2.7		25.3	
Râmnicu Sărat (RO)	max	29.9	4.6	36.7	6.2	41.4	2.4	38.5	1.6	489.2	15.1
	min	7	4	22.8	0.7	26.8	0.1	26.1	0.5	311	10.8
	Avg	15.5	1.1	29.7	1	35.2	0.8	34.5	0.7	425.1	9.8
	SD	5.2		4.5		3.8		3.1		46.1	
Roxolany (UKR)	max	27.3	4	55.2	4.2	51.5	0.9	40.9	0.9	464.6	15.7
	min	10.7	3.3	27.5	4	27.3	0.6	31.3	0.6	300.1	11.7
	Avg	20.3	1.3	35.6	2.1	36.1	1.5	36.5	1.3	391.3	11.5
	SD	4.9		12		5.8		2.5		42.9	
Stayky (UKR)	max	37.1	6.4	41.8	9	38.8	0.8	47	6.4	652.7	21.3
	min	14.1	4.4	21.6	2.4	22.5	0.6	24.8	4.4	329.4	15.2
	Avg	25.1	1.9	30.2	1.8	31.9	1.3	32	1.5	542.7	20.2
	SD	7.3		6.8		4.9		5.9		78.1	
Batainica (UKR)	max	38	3.9	54.3	8.6	54.6	1.5	53.8	1.5	567.5	19
	min	12.1	3.9	26.6	7.1	35.4	0.6	32	0.7	370.0	16.5
	Avg	20.6	1.3	40.5	1.4	41.4	1	39.9	0.9	457.4	9.2
	SD	6.6		6.5		4.9		4.8		44.2	

	max	28.9	8	33.5	6.6	48.3	2.6	48.6	1.5	671.7	19.3
Kuma	min	14.7	8.5	18.8	3.2	39.9	39.9	41.3	2	602.9	21.3
(USA)	Avg	22.7	1.7	26.2	1.8	43.5	0.9	44	0.8	629.2	8.7
	SD	4.7		5		2.5		2.3		24.5	
	max	27.9	3.4	45.1	4	48.1	1.5	54.3	0.4	715.3	17.6
Enders	min	17.4	4	28.9	4.1	39.6	1.2	38.5	1.7	390.3	19
(USA)	Avg	22.4	1	38.2	1.6	42.8	0.7	43.4	1.2	623.5	22.8
	SD	3.5		5.5		2.5		4.1		78.8	
	max	23.5	3.2	42.7	3.1	42.4	0.5	36.9	1.1	582.4	17.2
Baycaoyuan	min	11.6	2.7	29.8	0.5	37.1	0.6	31.6	0.7	466	14.9
(CHN)	Avg	17.2	1.4	37.2	1.5	39.6	0.6	34.8	0.6	523.6	11.2
	SD	4.4		4.7		1.8		1.8		35.5	

Table. 6.1. Descriptive statistics Radionuclides on the different loess accumulations

These differences may reflect the origin, age, weathering, erosion and deposition processes of the loess material, as well as the influence of environmental factors such as climate, vegetation and soil formation. The radionuclide activity concentration can provide useful information about the geochemistry of loess deposits, as well as their potential applications for environmental monitoring and assessment.

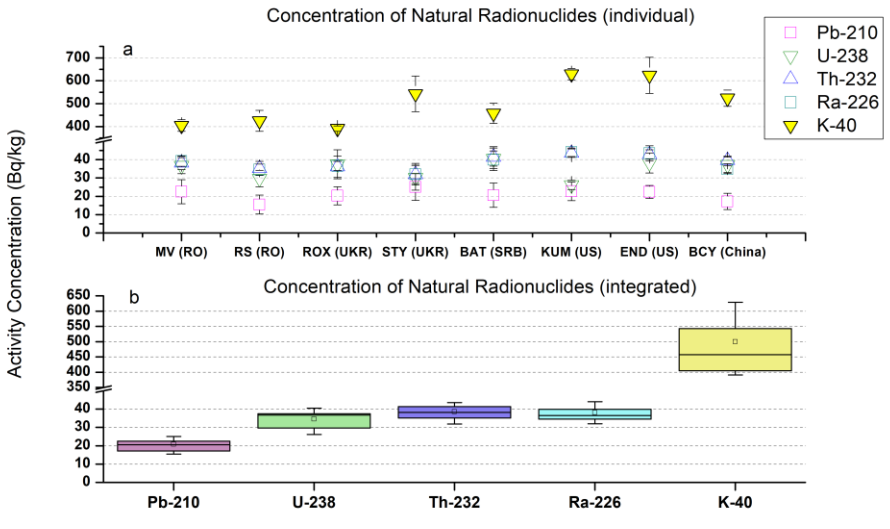

Figure 6.1. Individual (a) and integrated (b) concentration of natural radionuclide in loess deposits

The Box Chart (**fig. 6.1/b**) is a graphical tool used to visualize the distribution of ^{210}Pb, ^{238}U, ^{232}Th, ^{226}Ra and ^{40}K concentrations in all loess depositions. It shows that the largest deviation can be observed in the case of ^{40}K, which is largely influenced by the outlier results obtained from US loess samples. The ^{40}K activity concentration in loess depends on several factors, such as the provenance of the dust, weathering and pedogenic processes, and the moisture content of the loess. Generally, loess derived from glacial sources has lower ^{40}K activity than loess derived from desert sources, because glacial grinding reduces the potassium content of the rocks. (Ryzner 2020, Li 2020).

The activity concentration of ^{238}U, ^{232}Th, and ^{226}Ra in all studied loess deposits was found to be comparable, with no significant outliers. The activity concentration of these isotopes ranges between 26.2 and 40.5 Bq/kg for ^{238}U, 31.9 and 43.5 Bq/kg for ^{232}Th, and 32.0 and 44.0 Bq/kg for ^{226}Ra. The solubility of ^{238}U, ^{232}Th and ^{226}Ra depends on their chemical forms and the physico-chemical conditions of the environment. In the perfect closed system, the ^{238}U, ^{226}Ra and ^{210}Pb have the same activity concentration via the secular equilibrium in the ^{238}U series. However, the deviation for ^{238}U was higher, which is likely due to the solubility of ^{238}U.

An intriguing aspect of the **figure 7.1.** is the ^{210}Pb/^{226}Ra equilibrium anomaly, which indicates that the activity concentration of ^{210}Pb is not identical to that of ^{226}Ra, as predicted by the secular equilibrium of the ^{238}U decay series in the theoretical close system. This anomaly could also compromise theaccuracy of OSL dating techniques. Therefore, it is important to identify the origin of the disequilibrium between ^{210}Pb and ^{226}Ra.

Disequilibrium between ^{210}Pb and ^{226}Ra refers to the situation when the ratio of ^{210}Pb to its parent ^{226}Ra is not equal to one, which is the expected value under equilibrium conditions. In this section, activity concentration ratios of Loess deposit ^{210}Pb and ^{226}Ra ranged from 0.45 to 0.8 on average, but only Stayky Loess deposition exceeded the average (**Fig. 6.2**). A sample t statistical hypothesis test was employed to compare the ^{226}Ra/^{210}Pb ratio, and the mean of the ^{226}Ra/^{210}Pb ratio (0.45-0.8) differed substantially from the test mean (Raymond 2015) at the 0.05 level. This suggests that the difference in concentration between ^{226}Ra and ^{210}Pb is quite large and could be influenced by the intense ^{222}Rn escape throughout geological eras and measurement issues.

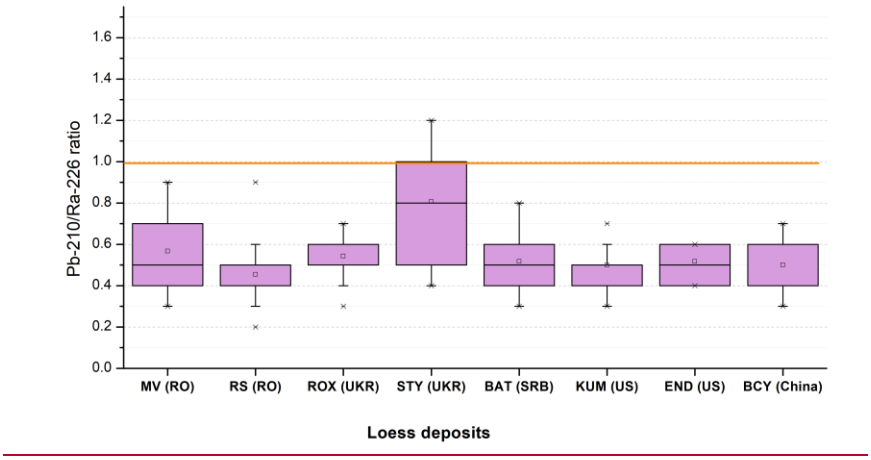

Figure 6.2. Averages of the ^{210}Pb *and* ^{226}Ra *ratio in the loess deposit*

Alpha spectrometry as described in Begy et al. (2015) was used to measure the concentration of ^{210}Pb in loess layers of Mircea Voda loess deposits This method was validated by analyzing six duplicates of IAEA-385 Irish Sea sediment. The difference between the received data ranged from 3.6 to 15%, with an arithmetic mean of 8.6% and an average ratio of 1.07. The concentrations of ^{210}Pb and ^{226}Ra in each layer were calculated and their ratio was displayed as a function of horizontal depth. **Figure 6.3** demonstrates that the ratio of ^{210}Pb to ^{226}Ra activity concentration declines linearly (r=0.91) as depth decreases, demonstrating that there is no equilibrium between ^{210}Pb and ^{226}Ra radio nuclides due to horizontal radon diffusion. The equilibrium between ^{210}Pb and ^{226}Ra is established at around 280 cm horizontal depth.

7. Final conclusions

We have applied gamma and alpha spectrometry for determining environmental radionuclides in various sedimentary environments. The study of different isotopes, their behavior in sediment columns and the use of peat moss as a climate reconstruction tool has provided valuable insights into climate variability and environmental change. It was demonstrated that the ^{210}Pb and ^{210}Po radionuclides show different behavior in the sediment columns. ^{210}Pb is relatively stable and can be used as a tracer of sediment accumulation rates, while ^{210}Po is more mobile and can be affected by the pH value of the water. The results suggest that when ^{210}P0 is used to determine the ^{210}Pb, the pH value of the water should be measured, since low pH can cause high ^{210}Po migration. This can lead to an underestimation of the ^{210}Pb activity and hence the

sedimentation rate. Therefore, it is important to consider the environmental factors that can influence the ^{210}Po distribution in the sediments when using this method.

The research delves into the sedimentation rates of specific lakes in Romania, noting changes across four main periods and relating these shifts to significant events like the construction of the Iron Gates power plant and changes in political regime. The lakes exhibited varying responses to these events, largely based on their proximity to the main branches of the Danube or local influences such as floods and storms. Furthermore, human activities, including industrial pollution and deforestation, have left their marks on sedimentation rates and heavy metal concentrations in these water bodies.

The study presents a novel, efficient method for alpha-spectrometric detection of ^{210}Pb in peat samples, evaluating the accuracy and reliability of four chemical digestion methods.

The thesis further incorporates a gamma spectrometry analysis of loess deposits from the US, Europe, and China. The results highlight varied correlation coefficients among isotopes within these deposits, suggesting different degrees of relationship among these elements. In order to investigate the cause of the ^{210}Pb ^{226}Ra ratio problem, the distribution of ^{210}Pb concentrations in the horizontal layers of the Mircea Voda loess deposits provides evidence that the equilibrium between ^{210}Pb and ^{226}Ra radionuclides is caused by horizontal ^{222}Rn emission. The equilibrium between the ^{210}Pb and ^{226}Ra radionuclides is established at a horizontal depth of 280 cm. If further confirmed, this result should have implications for sampling procedures as well as annual dose estimation procedures currently used by the luminescence dating community.

In conclusion, this multidisciplinary study brought contributions on the behavior of isotopes and their use for unravelling sedimentation processes. The data obtained can be used for future understanding climate dynamics, environmental changes, and their long-term impacts. These findings contribute to the advancement of scientific knowledge and can be utilized in various fields such as climate modeling, environmental monitoring, and sustainable development strategies. Further research directions and collaborations can build upon these conclusions, paving the way for a deeper understanding of our dynamic environment.

8. References

Appleby PG. 2001. Chronostratigraphic techniques in recent sediments. In: Smol JP, Birks HJ and Last WM ,Eds., Tracking environmental change using lake sediments, volume 1: Basin analysis, coring and chronological techniques. Springer: 171–203, DOI 10.1016/S0341-8162(78)80002-2

Appleby, E.D., Oldfield, E.D., 1978 The calculation of lead-210 dates assuming a constant rate of supply of unsupported ^{210}Pb in the sediment Catena, 5, 1-8.

Avram, A., Constantin, D., Veres, D., **Kelemen, S.,** Obreht, I., Hambach, U., Marković, S.B., Timar-Gabor, A., 2020. Testing polymineral post-IR IRSL and quartz SAR-OSL protocols on Middle to Late Pleistocene loess at Batajnica, Serbia. Boreas, 49 (3), 615-633.

Bačeva, K., Stafilov, T., Šajn, R., Tănăselia, C., Popov, S., (2011) Distribution of chemical elements in attic dust in the vicinity of ferronickel smelter plant - Fresenius Environmental Bulletin, 20 (9), 2306–2314

Begy, R.-Cs., Preoteasa, L., Timar-Gabor, A., Mihaescu, R., Tanaselia, R., **Kelemen, Sz**., Simon, H., 2016. Sediment dynamics and heavy metal pollution history of the Cruhlig. J. Environ. Radioact. 153, 167-175.

Begy, R. C., **Kelemen, Sz**., Simon, H., & Tănăselia, C., 2018. The history of the sedimentation processes and heavy metal pollution in the Central Danube Delta (Romania). Geochronometria, 45, 97-106.

Begy , R.-Cs., Dumitru, O.A, Simon, H., Steopoaie, I., (2014) , An improved procedure for the determination of ^{210}Po by alpha spectrometry in sediments samples from Danube Delta, J Radioanal Nucl Chem DOI 10.1007/s10967-014-3703-z

Coman, C., 2002. Danube Delta (Romania) – EUROVISION Case Study. pp. 21.

Constantin, D.,Veres, D., Anechitei-Deacu, V., Groza, S.M., Begy, R., **Kelemen, S.,** Buylaert, J.-P., Panaiotu, C., Hambach, U., Marković, S.B., Gerasimenko, N., Timar-Gabor, A., 2019. Luminescence age constraints on the Pleistocene-Holocene transition recorded in loess sequences across SE Europe–Quaternary Geochronology, 49, 71-77.

Figgins, P. E. (1961, January 1). THE RADIOCHEMISTRY OF POLONIUM. https://doi.org/10.2172/4034029

Flynn WW (1968) The determination of low levels of polonium-210 inenvironmental materials. Anal Chim Acta 43(2):221–227

Hakanson, L., 1977. An empirical model for physical parameters of recent sedimentary deposits of Lake Ekoln and Lake Vanera. Vatten 3, 266–289

Kelemen, Sz., Begy, R. Cs., Timar-Gabor A., Savin, C. F., 2023. Improving digestion methods for the determination of ^{210}Po by alpha spectrometry from peat bog samples. Manuscript submitted to Journal of Radioanalytical and Nuclear Chemistry, JRNC-D-23-00455.

Laszlo, F., 2007. Iron Gate Sediments Evaluation - Synthesis Report. pp. 99. UNDP-GEF Danube Regional Project. http://www.icpdr.org/main/resources/iron-gatesediments-evaluation-synthesis-report, Accessed date: 9 March 2018.

Li, Y., Shi, W., Aydin, A., Beroya-Eitner, M.A., Gao, G. (2020). Loess genesis and worldwide distribution. Earth-Science Reviews, 201, 102947.

Mabit L., Benmansour M., Abril J.M., Walling D.E., Meusburger K., Iurian A.R., Bernard C., Tarjan S., Owens P.N., Blake W.H., Alewell C., 2014. Fallout ^{210}Pb as a soil and sediment tracer in catchment sediment budget investigations: A review, Earth-Science Reviews, 138:335-351.

Miley SM, Payne RF, Schulte SM, Finn E (2009) Polonium–lead extractions to determine the best method for the quantification of clean lead used in low-background radiation detectors. J Radioanal Nucl Chem 282(3):869–872

Raymond S. Bradley, in Paleoclimatology (Third Edition), 2015

Ryzner, K., Nett, J., Zeeden, C. (2020). Desert loess: formation, distribution, geoscientific value. EGU Blogs - Stratigraphy, Sedimentology and Palaeontology.

Sanchez-Cabeza J.A., Ruiz-Fernández A.C., 2012.^{210}Pb sediment radiochronology: An integrated formulation and classification of dating models, *Geochimica et Cosmochimica Acta* 82: 183-200.

Saravana Kumar, U., Navada, S., Rao, S., Nachiappan, R., Kumar, B., Krishnamoorthy, T., Jha, S., & Shukla, V. (1999, July). Determination of recent sedimentation rates and pattern in Lake Naini, India by 210Pb and 137Cs dating techniques. *Applied Radiation and Isotopes*, *51*(1), 97–105.

Seiner BN, Morley SM, Beacham TA, Haney MM, Gregory S, Metz L (2014) Effects of digestion, chemical separation, and deposition on ^{210}Po quantitative analysis. J Radioanal Nucl Chem. doi:10.1007/s10967-014-3255-2

Szarlowicz K., Reczynski W., Misiak R., Kubica B., 2013. Radionuclides and heavy metal concentrations as complementary tools for studying the impact of industrialization on the environment, Journal of Radioanalytical and Nuclear Chemistry, 298:1323:1333.